Université de Montréal

Predicting Scleral Lens Rotation Based on Corneoscleral Toricity

Par

Gabriella Courey

École d'optométrie

Mémoire présenté en vue de l'obtention du grade de maîtrise
en sciences de la vision, option sciences fondamentales appliquées/cliniques

Avril 2021

Université de Montréal

École d'optométrie

This memoir, titled

Predicting Scleral Lens Rotation Based on Corneoscleral Toricity

Presented by

Gabriella Courey

Evaluated by a jury made up of the following members:

Pierre Forcier, OD, MSc

President

Langis Michaud, OD, MSc

Research Director

Jean-Marie Hanssens, OD, PhD

Jury Member

Sommaire

L'orientation des lentilles sclérales devient extrêmement importante pour maximiser la stabilité et la vision chez des patients qui portent des lentilles ayant une face antérieure torique. Les techniques cliniques actuelles pour déterminer la rotation d'une lentille sclérale impliquent l'utilisation de lentilles diagnostiques; cependant, ces méthodes nécessitent beaucoup de temps de chaise pour obtenir un ajustement optimal. Des appareils novateurs existent maintenant pour évaluer la forme de la surface oculaire et peuvent s'avérer utiles pour prédire la rotation des lentilles sclérales et augmenter l'efficacité globale des ajustements. Le but de cette étude comparative et randomisée était d'évaluer la rotation des lentilles sclérales en se basant sur des valeurs fournies par deux topographes. Quinze participants ont été recrutés et leurs deux yeux ont été imagés à l'aide de deux topographes: le Eye Surface Profiler (ESP) et le Cornea Sclera Profile (CSP). Les participants ont ensuite été ajustés avec la lentille OneFit MED dans un oeil et la Zenlens dans l'autre. La rotation de chaque lentille a été évaluée à l'aide de la lampe à fente et comparée à l'axe le plus cambré de l'astigmatisme conjonctival identifié par chaque topographe. Bien que les rotations des deux instruments ne soient pas comparables, l'ESP a prédit une rotation à moins de 15° de l'observation à la lampe à fente, ce qui la rend cliniquement acceptable pour les lentilles avec de faibles valeurs de puissance cylindrique. L'acuité visuelle des patients portant des lentilles avec des quantités élevées de toricité pouvant être plus affectée par la quantité de rotation, les ajustements empiriques semblent, à ce stade, être déconseillés pour ces cas.

Mots clés: Lentille sclérale, topographie, cornée, lentille de contact, segment antérieur

Abstract

Scleral lens orientation becomes extremely important to maximize vision and lens stability in patients who are fitted in front-toric lenses. Current clinical techniques to determine the rotation of a scleral lens involve the use of diagnostic lenses; however, these methods require a substantial amount of chair time to achieve an optimal fit. Contemporary equipment exists to evaluate ocular surface shape, which could be useful in predicting scleral lens rotation and increasing the overall efficiency of scleral lens adjustments. The goal of this comparative and randomized study was to evaluate scleral lens rotation based on the values provided by two scleral topographers. Fifteen participants were recruited and both eyes were imaged using two scleral topographers: the Eye Surface Profiler (ESP) and the Cornea Sclera Profile (CSP). Participants were fitted with the OneFit MED on one eye and the Zenlens on the other. Each lens's rotation was evaluated at the slit lamp and compared to the steep axis of conjunctival astigmatism identified by each topographer. While the rotations from both instruments are not comparable, the ESP predicted rotation within 15˚ from slit lamp observation, which makes it clinically acceptable for lenses with low values of cylindrical power. The visual acuity of patients wearing lenses with a high amount of toricity may be affected by the amount of rotation and are not suitable for empirical fittings at this point in time.

Key words: Scleral lenses, topography, cornea, contact lens, anterior segment

Table of Contents

List of Tables

List of Figures

List of Initials and Abbreviations

AOSS	Anterior Ocular Surface Shape
CSJ	Corneo-Scleral Junction
CSP	Cornea Sclera Profile
ESP	Eye Surface Profiler
FLF	First Lens Fit
FR	Fluid Reservoir
FRT	Fluid Reservoir Thickness
GP	Gas Permeable
HOA	High Order Aberrations
LZ	Landing Zone
MDF	Midday Fogging
OCT	Optical Coherence Tomography
PFD	Primary Functional Diameter
RA	Residual Astigmatism
SL	Scleral Lens

Chapter 1: Scleral Lenses, A Literature Review

1. History of Scleral Lenses

Scleral lenses are increasing in popularity with their plethora of new designs and contemporary fitting techniques. However, their use to correct ocular abnormalities is not a new occurrence.

The first true SL was conceptualized by the Muller brothers in the 1800s.(1) This lens made of blown glass polymers did not contain an optical power and did not have a goal of correcting vision; in fact, this first prototype's purpose was to protect the cornea from external damage. Today, this can be translated to the benefits of modern SL for patients with severe ocular surface disease or other corneal irregularities requiring ocular surface protection. Two years after the Muller brothers proposed their model in 1887, Adolf Fick(2) added the concept of optics to these SL, which could now correct vision. Shortly after this time, the Muller brothers, Fick and Kalt each developed SL with an optic zone to correct vision such as high myopia and to correct vision in patients with keratoconus, marking the beginning of SL to treat complex refractive error and corneal ectasia.(3, 4)

These first accounts of SL made with blown glass did not survive long with the growing use of new material in contact lens manufacturing, namely PMMA, in the 1930s. This lens material was deemed superior due to its high quality and the fact that it was easily produced. However, with the conception of corneal PMMA lenses, the side-effects of PMMA SL such as hypoxia deemed them almost obsolete.(5) In fact, the reason SL re-entered the market is largely due to the development of new materials. In 1983, Dr. Ezekiel(6) led the re-surgency of this movement among other pioneers with his article on oxygen-permeable SL which were more comfortable and tolerable for patients. With the invention of high-Dk materials in the 2000s, and the development of innovative manufacturing automated processes, SL fitting and wear sored in popularity and innovation in the field has been thriving ever since.

2. Indications for Scleral Lens Wear

There are two main groups of patients who are candidates for modern, gas-permeable SL: they can either be used as medical devices for rehabilitation of diseased corneas, restoration of the ocular surface or can likewise be fitted on normal corneas to compensate for refractive errors as well as patients suffering from ocular surface disease. If fitted correctly, these lenses have been described to provide both long- and short-term comfort with the visual benefits provided by small GP lenses.(7) Because of their fluid reservoir (FR), which serves, in part, to regulate very irregular corneal surfaces, SL can offer patients a significant improvement in vision which could not be achieved with regular ophthalmic corrections such as glasses or soft contact lenses.(8) The fact that the lens has no direct contact with the anterior ocular surface has several potential benefits. More specifically, patients may be more comfortable in SL since there is no direct contact with corneal surface as well as limited lid-to-lens interactions. Cases of warpage and damage to corneal epithelial cells are less common compared to GP lenses, however some cases have been described.(9, 10)

Indications for SL include vision restoration and correction in both adult and pediatric patients as young as 7 months old(11) with corneal irregular surfaces or ocular surface protection and treatment. Oftentimes, conditions such as keratoconus, keratoglobus and pellucid marginal degeneration are treated with SL, seeing as these conditions often result in irregular astigmatism that may not be correctable with glasses.(12) As well, patients having undergone refractive surgery or who have had corneal trauma are conditions which necessitate SL use.(13) By maintaining the moisture of the ocular surface through their FR, these lenses are extremely useful in patients with ocular surface disease including more severe cases, such as Sjögren's syndrome, Stevens-Johnson syndrome, graft-versus-host disease, and neurotrophic corneal disease.(12-15) This fluid layer contributes also to correct, at least in part, corneal anterior surface irregularity and optically induced aberrations.(8) Because of the comfort they provide, and their efficacy to correct visual acuity, they are also becoming an option for healthy corneas when other contact lens modalities fail to provide the desired visual acuity and comfort.(12)

Novel medical applications have also been outlined in more recent literature. Keating *et al.* described the successful use of anti-vascular endothelial growth factor molecules in the FR of a SL to treat corneal neovascularization.(16) Rehabilitation of exposure keratopathy resulting from periorbital thermal injuries with the use of SL has also been described in the literature.(17) For patients suffering from persistent epithelial defects refractory to standard treatment, the use of continuous wear SL along with the addition of a non-preserved antibiotic in the FR has shown promising results to heal the cornea.(18) These are only a few examples of the future of SL fittings and the benefits on both comfort and vision levels that they provide to patients.

With SL at the forefront of contact lens technology, there is a larger percentage of the general population that clinicians will need to adjust. This highlights the need for fitting techniques to be optimized and efficient without compromising patient safety and satisfaction.

3. Fitting Scleral Lenses

Knowing that SL present a great benefit to patients with corneal ectasia or other medical conditions, it is important to understand fitting principles of SL how these lenses uniquely provide uniformity to the ocular surface. Unlike a soft contact lens which sits on the cornea and lands near the limbus, a SL vaults over the entire corneal and limbal surface while its edges land on the soft, smooth conjunctival tissue.(19) The previous definition has led experts in the field to remove previously-instated scleral lens classification by size, since, regardless of their diameter, the fitting principle remains as explained above.(20) The area of vault between the eye and the lens is referred to as the lens' fluid reservoir (FR). This FR can be affected by a number of factors: the lens design (centration(21) and settling over time(22)), the elevation of the ocular surface(23) and the practitioner's fitting philosophy.(24)

3.1 Scleral Lens Anatomy

Understanding SL anatomy is a key element in successfully fitting a SL depending on each patient's specific case. The lens' basic anatomy can be divided into three main zones.(20) The first is the optic zone most commonly located in the center of the lens (or elsewhere in particular cases of decentered optics); this zone is the area of optical correction as well as the central FRT. After this, the transition zone denotes the area of transition between the optic zone and the landing zone, commonly found at or near the limbus depending on the patient's ocular anatomy. This zone can be modified if limbal vault is excessive or insufficient and changes in this zone can modify central FRT. Finally, the landing zone (LZ) describes the zone where the scleral lens "lands," or, more precisely, aligns, on the conjunctival/scleral surface. It is important to note that the LZ starts from the primary functional diameter of the lens, meaning the chord of the first point of contact where the lens touches the ocular surface, and ends at the lens' edge. In fact, the LZ bears the weight of the SL; therefore, its proper alignment with the patient's ocular shape is of the utmost importance for a successful fit.

The LZ can be customizable according to the patient's ocular shape.(25) For eyes that have a relatively symmetrical shape, a spherical LZ could be adequate. However, a back-surface toric LZ can also be ordered if the lens-sclera interaction is not acceptable because of either compression or elevation. Here, there is an important distinction to make between concepts: while front-surface toricity refers to optics included in a lens to compensate for residual astigmatism, back-surface toricity does not refer to optics like bi-toric corneal gas-permeable lenses but refers to the anatomy of the landing zone.(26) In more specific cases where ocular surface shape varies significantly causing an inacceptable edge in multiple quadrants, a quadrant-specific LZ is necessary.

3.2 Anterior Ocular Surface Shape (AOSS)

Before discussing the details of AOSS, it is necessary to understand the concept of sagittal height as related to the eye and parallel this information to the sagittal depth concept used to characterize SL. The definition of sagittal height outlines the distance from a line joining the extremities of a curve (chord) to the apex of said curve, while the term toricity is described as the greatest difference in sagittal height between two meridians regardless of their positioning. Applying this concept to the cornea, a significant piece of information to note is that sagittal height, often described in μm, increases as the chord increases.(27) This notion is crucial when considering the fitting principles required for SL. When fitting a soft contact lens, the corneal sagittal height needs to be considered; however, scleral lens adaptation requires a unique understanding of the corneal as well as the scleral sagittal height values to have an adequate fit.

Figure 1: A Representation of the Sagittal Depth of a SL, adapted from Dr. Hall(23)

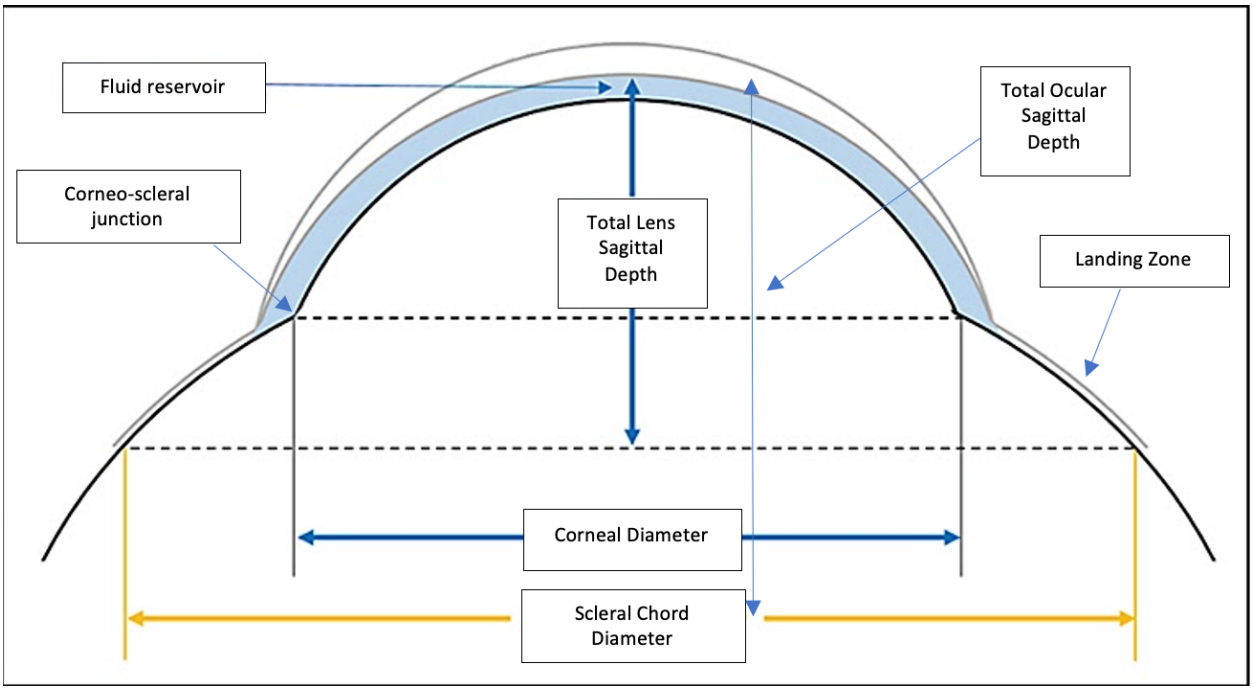

AOSS, or corneo-scleral anatomy, is crucial when aiming to understand how the lens lands on the surface of the eye. Factors which influence scleral lens apposition on the ocular surface include the corneo-sceral profile, the corneo-scleral junction angle, the diameter of the lens as well as the height of the tear film reservoir.(28)

Previous studies have aimed to described AOSS in the general population. The corneo-scleral profile has been described as a non-rotational asymmetric surface with irregularities varying from patient to patient.(29) DeNaeyer *et al.*(30) conducted a study analyzing the AOSS of 144 eyes of potential scleral lens wearers in an aim to provide a classification for scleral shape patterns. In their study findings, the authors found that only 1/3 of the eyes had regular symmetrical scleral patterns, whereas 2/3 of the data collected showed signs of irregular patterns of asymmetry, a conclusion that demonstrates that the regular lenses with spherical haptics, used by most clinicians as diagnostic lenses in their practice, would only adequately fit 1/3 of the clinical population. This is an important finding for SL practitioners, as it sheds light on the asymmetry of the AOSS and the subsequent necessity for more specialized lens designs. Even more, the same authors conducted a similar study,(31) however this time evaluating the scleral shape of participants with corneal ectasia as compared to that of normal corneas. The authors found that participants with corneal ectasia showed significantly different scleral shape patterns that those of normal eyes. While non-ectatic eyes tended to present more rotational symmetry, larger amounts of scleral toricity were noted in the ectasia group, even more so when ectasia was more than 1.25mm from the corneal apex. Moreover, Consejo *et al.*(32) discovered that corneal and scleral asymmetry are highly correlated in astigmatic eyes, suggesting once again that toricity should be viewed on the eye as a whole rather than simply on a corneal level. Considering the fact that a large percentage of patients fit in scleral lenses are patients with either corneal ectasia or regular/irregular astigmatism, their increased amount of scleral toricity only further underscores the need for clinicians to pay more attention to scleral shape in order to avoid the consequences of an inadequate fit.

As well, in her study on the influence of scleral shape on scleral lens design, Fadel(28) highlights the fact that different scleral shape patterns require different landing zones for the lens to have a proper alignment and relationship with the sclera. This is due to the fact that a lens that is not adequately adapted will not be stable on the conjunctival surface. This will lead to lens decentration with physiological impacts, such as lens compression, or optical impacts, such as the misalignment of the optical and visual axis as well as the induction of a prismatic FR. These fitting problems need to be remedied and this requires a concrete understanding of the AOSS, without which many trial-and-error troubleshooting techniques are required and often result in many lenses unnecessarily being ordered from manufacturing companies and increased chair time. Considering the results of the previous study by Denaeyer *et al.,*(30) custom landing zones such as toric, quadrant-specific designs or even impression-based lenses would be necessary for over half the clinical population requiring scleral lenses. It is therefore increasingly important to understand how these lenses stabilize on the eye to avoid multiple lens exchanges.

The CSJ angle also affects the way a SL lands on the ocular surface. A study(33) exploring the CSJ angle on 8 meridians using OCT imaging revealed that measurements of CSJ angle were relatively symmetrical within a 15mm diameter; however, beyond this point, the asymmetry of the CSJ angle measured suggests that toric or quadrant specific LZ should be considered beyond 15mm of diameter. This is also important when considering the diameter of the scleral lens that is to be adjusted; larger scleral lenses will often require toric peripheries. As well, multiple studies(29, 34) have demonstrated that the CSJ angle is sharper nasally than it is temporally, which may explain lens decentration as evident by a smaller nasal sagittal height value. Moreover, it has been demonstrated that lenses with larger central FRT tend to have larger amounts of decentration,(35) directly affecting the integrity of the lens's edge on the sclera.

3.3 Instrumentation to Measure AOSS

Contemporary instrumentation exists to map the corneo-scleral profile. The Eye Surface Profiler (Eaglet Eye, Netherlands), a specialty instrument based on Fourier transform profilometry, has been demonstrated to adequately map the ocular surface.(36, 37) Recently, The Pentacam (Oculus, Germany) has implemented an algorithm called Cornea Scleral Profile to aid in scleral lens fittings. This algorithm provides data from Scheimflug imaging to gather information about ocular sagittal height. While the ESP has been studied in the past as an effective tool to map AOSS,(36) the Pentacam's relatively new software merits to be evaluated since it is more widely found in clinical settings across Quebec and Canada. For the purpose of this study, the ESP and the CSP will be used to collect information about AAOS. Please see Chapter 2, section 3.2 for further information on both these instruments.

3.4 Fitting Process

The global consensus on concrete guidelines for SL fitting techniques have been very recently established for the first time in a series of articles published on March 25, 2021.(38) Therefore, since this literature is extremely novel, practitioners still fit their SL based on a specific lens' fitting guide or based on the clinician's personal preference developed from their clinical experience. However, the principles of fitting SL have always been globally based upon two main pillars: vaulting the cornea and the limbus all the while achieving an optimal lens alignment with the ocular surface.(12)

In clinic, practitioners often use a set of diagnostic lenses to achieve an optimal fit, with an initial lens chosen based on the flat keratometry value on the axial map or the best fit sphere on the elevation map of corneal topography, all of this depending on each lens' specific fitting requirements. In fact, the rule of thumb in cases where measuring the ocular sagittal height is not possible is to consider that a non-ectatic eye has an ocular sagittal height of roughly 3800-4000μm,(39) and to increase this amount if fitting a

keratoconus patient or decrease this amount if fitting an oblate cornea. Certain manufacturers will even recommend starting off with the lens at the center of the trial set.

By trial-and-error technique, clinicians try lenses until they achieve an ideal fit centrally and peripherally. Central FRT is determined using the slit lamp technique or, if available, by anterior segment OCT. With diagnostic lenses, clinicians evaluate the alignment of a lens as well as the behavior of its edges (such as compression, impingement or edge lift), which highlight misalignment with the corneal or conjunctival surface that need to be compensated. This technique is widespread, but often requires more chair time and increased lens modifications. Understanding how the LZ interacts with the conjunctival surface is therefore extremely important in a successful fit. Up until recently, little data was known on anterior ocular surface shape, its irregularity and the consequent effects on SL fits.

4. Fitting Complications

If the SL is not properly adapted and does not align well with the ocular surface, fitting challenges and complications may arise that require adjustments to specific zone. As a matter of fact, the behavior of a lens on the surface of the eye varies throughout the course of the day: the central FRT diminishes(22, 40, 41) and the spongy, moldable conjunctival tissue can get compressed by the lens' weight.(42) As mentioned previously, lens decentration may also occur during the day, usually in the inferior-temporal direction. While inferior decentration is likely attributed to the interaction between the eyelids and the lens as well as central FRT,(9) horizontal decentration can be linked to anterior ocular surface shape asymmetry. The nasal sclera has been demonstrated to be flatter and more elevated than the temporal sclera,(43) which causes the lens to move to the point of least resistance: temporally. These fitting challenges highlight the need for a proper LZ to ocular surface relationship; thus, it is of keen importance to understand and accurately map AOSS to minimize these problems.

As previously discussed, custom LZ are more often than not necessary to adequately fit patients and minimize complications. When the LZ of a scleral lens is not adequately aligned with the ocular surface, multiple problems can arise causing discomfort to the patient and sub-optimal visual outcomes.(44) A misaligned LZ can cause blanching as well as lens edge elevation leading to increased awareness of the lens on the eye. Moreover, midday fogging, a concept which describes the accumulation of debris such as leucocytes, lipids and mucine inside the FR(45) and has been recorded in 20-33% of all SL wearers,(44) results in the chief patient complaint that they need to remove their lens after few hours of wear and clean it due to blurry vision. The etiology of MDF is difficult to pinpoint, but past studies have attempt to describe the factors which may contribute to its onset. One theory is that MDF may be related in part to a misaligned LZ-to-ocular-surface relationship, causing debris to accumulate in the FR.(46) For eyes that have irregular conjunctival shapes, toric or quadrant specific LZ may be an interesting option to limit MDF for these patients. Another theory describes the importance of the central FRT as one of the most crucial factors in controlling MDF. In fact, it has been demonstrated that the amount of leucocytes in the FR increases two-fold every 50 microns above a central FRT of 200 μm.(47) This suggests that minimizing MDF would require SL adjustments with central FRT equal or less than 200μm without any corneal contact. Limbal FRT has also been hypothesized to contribute to MDF; lenses with a minimal FRT at the limbus allow for less debris to enter and cloud vision.(48)

As well, conjunctival prolapse or inlapse can arise from an inadequate LZ.(49, 50) This phenomenon describing the migration of conjunctival tissue onto the peripheral cornea adjacent to the limbus has been described to appear because of the sub-atmospheric hydraulic forces under a SL(44) and a larger gap existing between the inferior limbus and the lens. This does represent a fitting challenge for practitioners because, although relatively benign on the short-term,(51) the long-term effects of potential limbal or conjunctival neovascularisation caused by the prolonged presence of conjunctival tissue on the cornea have yet to be described.

Moreover, if the LZ is not correctly aligned with the ocular surface, the lens can be either decentered or experience flexure depending on the diameter and thickness of the lens.(28, 52) Both decentration and flexure compromise the patient's visual acuity in cases where precise vision is required, for example cases of multifocal SL or lenses with front-toric designs.(8, 53, 54) As previously mentioned, a scleral lens will always tend to decenter in the inferior, temporal, or inferior-temporal direction due to its mass as well as the conjunctival profile.(55, 56) If lens decentration is excessive and the lens is fit with a high FRT, a prismatic effect is caused by the uneven and non-uniform tear reservoir resulting in altered optics, in the form of high order aberrations, which is wrongly confounded with residual astigmatism.(52)

When a lens is properly adapted with a uniform tear reservoir and an adequate LZ, RA is not a common problem encountered by clinicians. However, RA may be the result of lens decentration, uncorrected HOAs or lenticular astigmatism,(57) and less commonly a result of lens flexure as previously hypothesized.(57) In cases with persistent RA which limits the patient's visual acuity, this astigmatism can be corrected using front-toric lens designs; in other words, the RA is corrected with a toricity which aims to increase optical performance. As if the case with soft toric lenses, lens stabilization is of the utmost importance to maintain clear vision for toric SL. Stabilization is also of prime importance if lenses are designed to compensate for ocular HOA.

SL stabilization is achieved by incorporating back-surface toricity into the lens to align it with the ocular surface. A proper prediction of this alignment is extremely important in cases of front-toric lenses and HOA-compensated designs, as it ensures precise and stable vision. Much like soft lenses, misaligned SL will cause visual discomfort and dissatisfaction.(58) However, SL stabilization is quite difficult to determine since their adjustment relies primarily on the relationship between the lens and the anterior ocular surface shape (AAOS).

5. Contemporary Dilemmas

There are not many private practitioners who have access to instruments which are capable of accurately mapping AAOS. Fitting SL is done using a diagnostic set. If the lenses in the diagnostic set have spherical LZs, scleral shape can be estimated by looking at the areas where the LZ is tight (compression, suggesting a flat scleral surface) or where the LZ is loose (excessive edge lift, suggesting a steep scleral surface). Evidently, this technique could take a substantial amount of chair time seeing as many refits could be necessary. Moreover, if practitioners have advanced diagnostic sets with known toric haptics, this facilitates the fitting process because both the steep and flat meridians are known and the practitioner can better communicate the fitting specifications to the laboratory. Based on their design, toric scleral lenses will usually place themselves in the area of least resistance on the sclera; therefore, along the steep meridian of the sclera. However, even in these cases, many modifications are sometimes required to achieve a successful fit, seeing as we know that AAOS if often not simply spherical or simply regular toric.

Thus, this study will examine whether it is possible to accurately determine the rotation of a SL using measurements of AOSS from two corneoscleral topographers.

Chapter 2: Predicting Scleral Lens Rotation Based on Corneoscleral Toricity

Personal Research Contribution

1. Introduction

When SL are used, in regular or irregular corneas, refractive error is habitually well compensated. However, in some cases, RA is found as a result of lens decentration and FR shape, lenticular astigmatism(57) or more rarely, lens flexure. The presence of non-corrected HOA, mostly coma, may be generated as a result of refractive indices change between air, lens material, FR and cornea.(59, 60) HOAs impact the quality of visual acuity, mimicking the presence of RA. When RA is present, it requires the use of front toric lens designs to improve visual acuity of the patient.

As is the case with soft toric contact lenses, front-toric scleral lenses need to be stable in order to optimize vision. As well, any of their rotation on the ocular surface must be compensated. Soft lens position is influenced by the corneal profile, the lid tension, the lid to lens interaction, the interpalpebral aperture and the orientation of the canthus.(61) It relates also to the sag depth of the lens versus the ocular sagittal height,(27) as well as the movement and the subsequent comfort of said lens. Soft lens rotation may be compensated with the use of several mechanisms. Technology has improved since the conception of the narrow prism ballast technique, which was actually not so effective. Today, modern stabilization processes, relying on several mechanisms like enlarged prism with thickness profile control, make it easier to compensate for soft lens rotation. However, this process is more challenging for SL. Part of this challenge is the fact that we do not know much about the real lens-to-conjunctival surface interaction.

One element we know is that the rotation of these large lenses is mostly influenced by conjunctival/scleral shape, also known as AOSS, which is considered a non-symmetrical surface. As demonstrated by previous studies,(28, 30, 31) more than 2 out of 3 patients present with a significant level of conjunctival irregularity and this irregularity varies from patient to patient.(30) Toricity is described as the greatest difference in sagittal height between two meridians regardless of their positioning. The level of toricity, its regularity,

and its orientation (axis) is not predictable from the corneal profile and is only determined when the ocular surface is mapped with modern profilometer.

Habitually, lenses tend to stabilize over the steeper meridian.(54) Without profilometry, the orientation of this meridian is not possible to detect through regular examination techniques. It is therefore difficult to predict the final rotation of the SL.

Another method is to apply diagnostic lenses, made with significant toric peripheral curves and marked. Manufacturers tend to mark lenses along the flattest meridian. One can estimate that the steepest meridian will be located 90 degrees apart, but 65% of the conjunctival surfaces present an irregular astigmatism which means that main meridians are not perpendicular but rather irregular, i.e. with non-perpendicular main meridians.(30)

Therefore, being able to evaluate more easily, clinically speaking, where the conjunctival steep meridian is located becomes essential to achieving successful and stable fits, especially when it comes to prediction SL rotation for lenses with front-toric designs.

2. Study Objectives

This study aims to evaluate the accuracy in which two contemporary SL topographers can empirically predict SL fitting (i.e. rotation, central FRT and lens compression) based on the analysis of the ocular surface profile. As a secondary goal, this study aims to evaluate the central FRT from the lens predicted by the Trial Lens Predicting system (*First Lens Fit* algorithm) of the of the ESP (Eaglet Eye, Netherlands) and compare it to the central FRT suggested by the fitting guides for two different SL designs.

3. Materials and Methods

3.1 Study Design

This randomized, non-dispensing, comparative study was approved by the Université de Montréal's Comité d'éthique et de la recherche Clinique (CERC) and adheres to the declaration of Helsinki. It was conducted by the main author at the Clinique Universitaire de la Vision.

After providing informed consent, subjects were assessed through several testing procedures to validate inclusion and exclusion criteria (See Annexe 1). Once determined that they met the inclusion criteria, the eligibility assessment was conducted. Oriented case history ensured that participants did not have any pre-existing ocular conditions and thus had normal ocular health. Following this, a slit lamp examination to observe the integrity of the ocular surface was performed with the use of sodium fluorescein. Any questions relating to the study or consent form were answered at this time and during the totality of the duration of the study.

Corneoscleral topography was performed on both eyes of each participant using two instruments (please see section 3.2 for the detailed description of each instrument). The CSP (Pentacam, Germany) measurement was always performed first seeing as this machine does not require the use of sodium fluorescein. In fact, the use of sodium fluorescein may affect the measurement capture of the CSP.(62) After the eyes were imaged with the CSP, the ESP (Eaglet Eye, Netherlands) was then used to obtain the images of corneoscleral topography.

Both the steep and flat sagittal height values and as well as their corresponding axis were determined using both instruments at a chord of 14 mm, 15 mm and 16 mm, as well as at the lens' PFD, the area where the lens first meets the ocular surface. This value was provided by the manufacturer. The choice to analyze this data at these main chords was

made in order to evaluate whether the steep meridian of AOSS toricity was stable depending on the chord.

For the purpose of evaluating the SL rotation, only the data at 15 mm and at the lens' PFD were used. The PFD was chosen to evaluate the relationship between lens rotation and the first point of contact of the lens on the ocular surface; the 15 mm location point was chosen because of increased AOSS toricity as of that chord as described in the literature.(33)

3.2 Instrumentation

3.2.1 Eye Surface Profiler (Eaglet Eye, Netherlands)

This instrument is an eye profiler of both the cornea and the sclera, which also offers imaging of the ocular surface up to 22mm beyond the limbus.(63) The ESP takes over 350,000 data points along the cornea and sclera to create the topography. This instrument also requires fluorescein so that the image of the tear film distributed over the ocular surface is projected back into the instrument as a mold. Generating this topography only requires one measurement, which comprises of 2 single shots in succession that both lasts a few milliseconds. The 3-dimentional model is then created based on these images which allow for viewing of the cornea, limbus and sclera. To create a composite eye, which was used in this study, a minimum of three measurements must be taken per eye. These measurements were then merged together, which made it possible to obtain a measure of conjunctival toricity.

Figure 2: Anterior Ocular Surface Shape Measurements Provided by the ESP

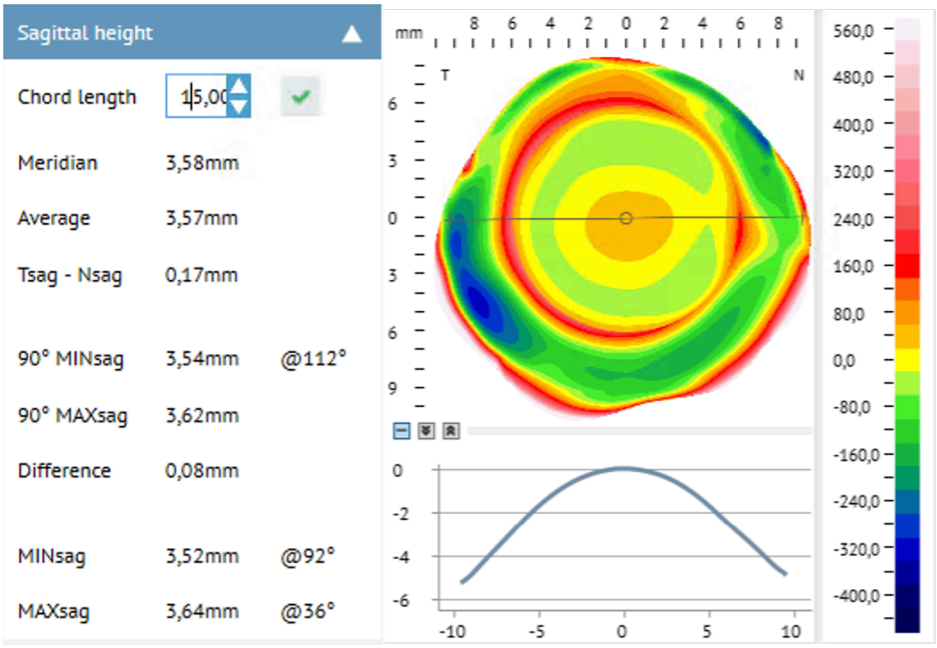

3.2.2 Cornea Scleral Profile (Pentacam, Germany)

This instrument uses the concept of Scheimpflug imaging to obtain measurements of scleral shape to aid in lens adjustments. Along with collecting the usual data that the Pentacam provides such as corneal information, the CSP can provide information on scleral shape up to 18 mm horizontally and 17 mm vertically.(63) This is done by taking 5 measurements while the patient is looking in primary gaze; one central measurement and 4 peripheral measurements. Each measurement obtains 50 scans for a total of 250 Scheimpflug images. Unlike the ESP, this measurement is anterior segment-independent, meaning that it does not require the use of fluorescein.

Figure 3: Anterior Ocular Surface Shape Information Provided by the CSP

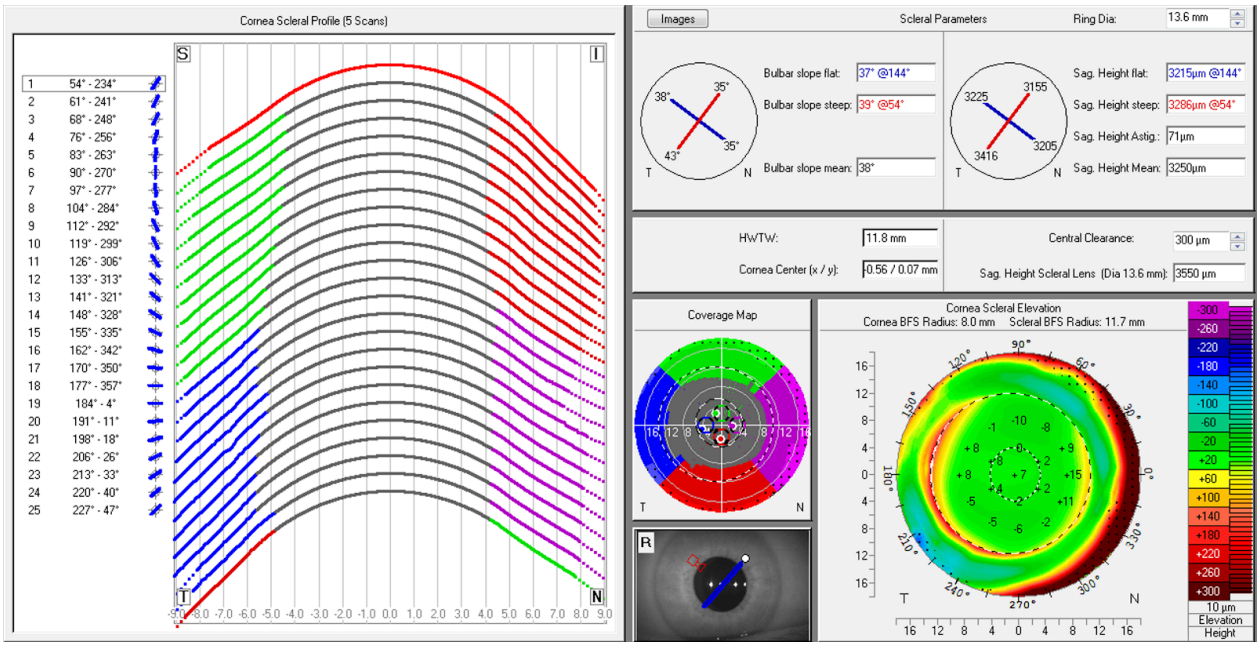

Table 1: Comparison of Features on both the ESP and the CSP

	ESP	**CSP**
Manufacturer	Eaglet Eye, Netherlands	Pentacam, Oculus, Germany
Measurement technique	Fourier-based domain Profilometry	Scheimpflug imaging
Image capture	1 image, by two blue-light fringe projectors and one centrally located camera with a yellow filter	5 images, 1 centrally and 4 peripherally
Ocular Surface Coverage	22 mm	18 mm horizontally, 17 mm vertically
Use of Fluorescein for Measurement	Yes	No
Composite Eye Option	Yes	No

3.2.3 Optovue i-Vue anterior segment OCT

In this study, anterior segment optical coherence tomography was evaluated using the Optovue iVue SD-OCT (Clarion Medical Technologies, Cambridge, Canada). This is a non-contact, high resolution (5μm) OCT that is also used to image the posterior segment of the eye. This OCT uses a scan beam length of 840±10nm. To evaluate the anterior segment, it is used to evaluate central corneal and epithelial thickness (6mm central diameter) as well as measurements of the iridocorneal angle. For the purpose of this study, the anterior segment OCT was used to evaluate the vaulting associated with each SL.

3.3 Lens Selection

The initial diagnostic lens was then determined using the *First Lens Fit* algorithm provided by the ESP. The right eye of the participants was randomly fitted with either the OneFit MED (L1) diagnostic lens (Blanchard Laboratories, Sherbrooke, QC) or the Zenlens (L2) diagnostic lens (Alden Optical, Lancaster, NY). The left eye was fit with the other lens. For example, if the randomization made it so that the right eye was fit with L1, then the left eye would automatically be fit with L2. See table 2 for a detailed explanation of lens parameters.

Table 2: Lens Parameters

	L1	**L2**
Overall diameter	15.6	16.0 mm
PFD	13.6 mm	12.8 mm
Sag depth	From 3800 to 6200 in 50μm increments	From 3200 to 6700 in 10μm increments
Peripheral curves	Toric Flat meridian: +75 Steep meridian: -75 Total difference: 150 μm	Toric (by 30 μm increments) Flat meridian: steep 2 Steep meridian: flat 3 Total difference: 150 μm
Average lens thickness	250 μm	300 μm
Material	Hexafocon A	Hexafocon A
Lens mark	On the flat meridian	On the flat meridian

Lenses with diameters greater than 15mm were used for this study knowing that conjunctiva is almost spherical up to 15 mm but becomes more and more toric as we go further away from the limbus. Both of these lenses are fitted by sagittal height value and have known simple toric peripheral curves (150 μm); therefore, their peripheral curves are separated by 90˚. The steep axis of rotation was determined by subtracting 90˚ from the observed rotation of the flat axis. Before application, the lenses were filled with sodium-hyaluronate based non-preserved artificial tears (i-drop pur gel, Imed pharma, Montreal, Quebec, Canada).

Initially after lens application, the lens' were evaluated at the slit lamp to make sure that they were fitted adequately. In other words, a quick evaluation under the slit lamp was done to make sure that there were no air bubbles, that the lens was not touching the cornea and that there was no excessive conjunctival compression or edge lift. After the

lens fit was validated, the horizontal markings were manually rotated by the examiner to align along the horizontal meridian and lenses were left on the patient's eyes to stabilize for 30 minutes. This amount of time has been demonstrated in the literature to allow for an accurate depiction of lens behavior after a day's wear.(22)

3.4 Lens Evaluation

After the lens stabilization period of 30 minutes, the rotation of both lenses was assessed by the main author. The axis of rotation (in degrees) was read directly off of the slit lamp. To facilitate measurement comparison with both topographers, the TABO measuring system used in optics was applied to the eye. Therefore, regardless of the eye examined, the 0˚ mark is always found on the right-hand side of the examiner while the 180˚ mark is on the left-hand side.

Figure 4: Example of the TABO measuring system applied to the left eye to measure SL rotation(64)

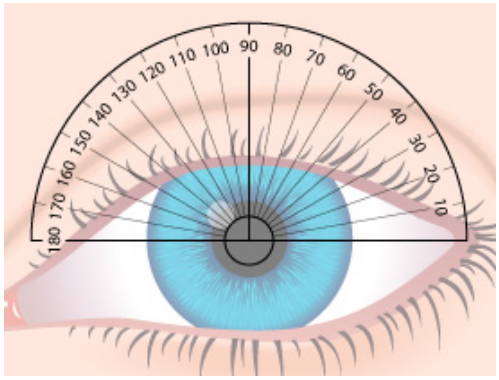

Since the lenses have two markings each at 180˚ from each other, this facilitated measurements. Therefore, if a lens rotated in the clockwise direction by, for example, 30˚, the superior lens marking was noted at 150˚. However, if the same 30˚ rotation was in the counterclockwise direction, the rotation was noted as 30˚. This same system was used for both the right and left eyes. Three measurements of rotation with 1-minute intervals

were taken and the mean rotation was calculated. The lenses were not moved between measurement readings

Following the evaluation of the lens's rotation, 3 anterior segment OCT images were taken per eye. Scans at primary gaze are required to evaluate the central vault of the lens with respect to the cornea, as the OCT is taken through the horizontal meridian. Nasal and temporal readings, at a 15˚ angle, are required to evaluate the landing zone of the lens and its interaction with the bulbar conjunctiva/sclera. Lens compression was evaluated with the nasal and temporal lens readings at the anterior segment OCT (see Figure 5). As demonstrated elsewhere,(50) a straight line (line A) was drawn from the surface of the conjunctiva directly through the edge of the lens. The lens' thickness was calculated, in microns as a line connecting point A to point C (line B) perpendicular to line A. The amount of compression, also in microns, was calculated by the distance between the line connecting point A to point B (line C). Lens compression was reported as a percentage (line C / line B). Clinically, the aimed percentage of lens compression is 50%,(65) meaning that half of the lens' thickness is compressed in the conjunctiva and the other half rests on the conjunctival surface. The lenses were then removed and a final slit lamp exam was performed to assess ocular health. Fluorescein was instilled to evaluate the presence/absence of any ocular staining under blue cobalt light using the yellow Wratten filter.

Figure 5: Lens compression method as evaluated through anterior segment OCT imaging (66)

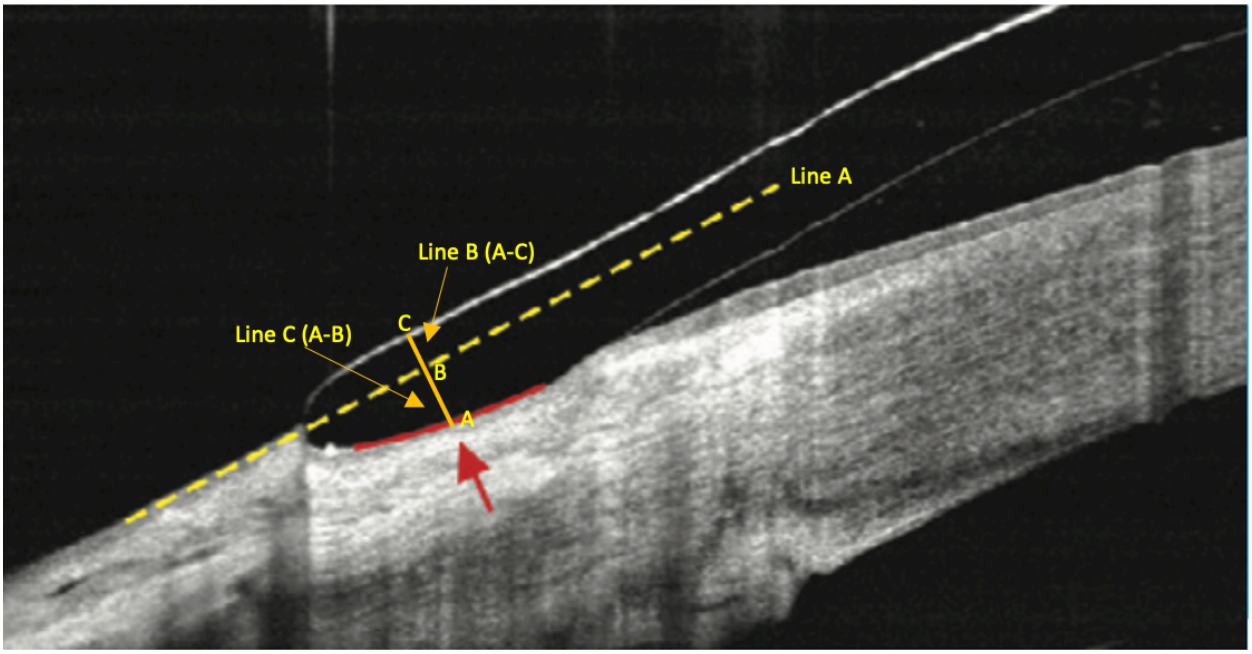

Table 3: Explanation of the variables in the present study

Variable	**Dependent/ independent**	**Quantitative / qualitative**	**Type of variable**	**Levels**
Topographer	Independent	Qualitative	Nominal	A or B
Lens	Independent	Qualitative	Nominal	L1 or L2
Steep axis of AOSS toricity	Independent	Quantitative	Continuous	Values in degrees (˚), 0-180
Rotation	Dependent	Quantitative	Continuous	Values in degrees (˚), 0-180
FR	Dependent	Quantitative	Continuous	Values in microns (μm)
Lens Compression	Dependent	Quantitative	Continuous	Values in percentage (%)

3.5 Statistical Analysis

To analyze the comparison of the predicted rotation from either topographer (Topographer A vs Topographer B) as compared to the observed rotation, a repeated-measures ANOVA was performed on the data with 2 factors: topographers (A and B) and lens (L1 and L2). The analysis was done at both a 15mm chord and at the lens' PFD. All rotations are exemplified by a mean difference, that is the mean difference between the observed rotation and the condition at which that is being compared. No clockwise or counterclockwise direction of rotation was noted as only the absolute values were analyzed in this study.

An analysis of the data was also performed by running a bivariate Pearson correlation as well as a Spearman correlation between different variables to evaluate their relationship with the accuracy of the predicted lens rotation.

4. Results

Statistical analysis was performed using SPSS software. Fifteen subjects, 67% female, aged between 21 and 33 for an average age of 25.13±3.52 years, completed the study. All subjects were asked to discontinue soft contact lens wear 48 hours prior to the study and none were prior SL wearers.

4.1 AOSS Characteristics

The mean values for AOSS toricity at different chords for topographer A are shown in the table below. This value describes the difference between the minimum sagittal height and the maximum sagittal height at a given chord, in microns.

Table 4: Descriptive statistics for AOSS toricity for topographer A, in microns (μm) categorized by Eye

	14 mm		15 mm		16 mm	
	OD	OS	OD	OS	OD	OS
Mean	154.00	182.67	190.00	221.33	231.33	264.67
Std. Deviation	74.24	84.47	84.68	87.17	101.76	113.57
Minimum	40.00	80.00	70.00	110.00	90.00	110.00
Maximum	310.00	370.00	390.00	430.00	450.00	520.00

The mean values for AOSS toricity in microns at different chords for topographer B are shown in the table below.

Table 5: Descriptive statistics for AOSS toricity for topographer B, in microns (μm) categorized by Eye

	14 mm		15 mm		16 mm	
	OD	OS	OD	OS	OD	OS
Mean	102.53	109.87	143.20	150.33	216.93	213.87
Std. Deviation	57.50	53.79	88.40	85.22	114.48	114.45
Minimum	11.00	40.00	7.00	32.00	24.00	45.00
Maximum	193.00	191.00	283.00	269.00	405.00	375.00

The mean difference between the values of AOSS toricity given by topographer A at 15 mm and the lens' toricity (150μm for each lens) was 73 μm±71.252.

4.2 Correlation Between Lens Toricity and AOSS Toricity

A Pearson bivariate correlation was done between the difference between the lens' toricity and the AOSS toricity (above) and the mean absolute differences in rotation. No significant correlation was found between these two variables (r=-0.002, p=0.991).

4.3 SL Fit Results

A summary of lens characteristics is found in Table 7. The suggested central FRT recommended by each manufacturer after 30 minutes is 200-225 μm for L1(66) and 300 μm for L2(67).

Table 6: Descriptive statistics of SL fit results

		N	Average	SD	Standard error	95% CI		Min	Max
						Inferior	Superior		
Central FRT (μm)	L1	15	189.20	82.76	21.37	143.37	235.03	64	325
	L2	15	405.67	113.40	29.28	342.87	468.47	194	598
% nasal compression	L1	14	53.52	7.43	1.99	49.23	57.82	42.80	71.43
	L2	15	46.82	8.53	2.20	42.10	51.55	25.72	57.94
% temporal compression	L1	14	61.83	8.06	2.15	57.18	66.49	45.61	77.20
	L2	14	54.36	6.86	1.83	50.40	58.32	45.34	70.00

There were statistically significant differences between values of central FRT ($F(1,29)=35.664$, $p<0.01$), nasal compression ($F(1,28)=5.047$, $p=0.033$) and temporal compression ($F(1,27)=6.981$, $p=0.014$) between L1 and L2.

4.4 Average rotation at a 15mm chord

For topographer A (ESP), the mean absolute rotation difference between the steep axis reported by the topographer at 15mm and the examiner-observed rotation was 12.42˚±16.93 for L1 and 13.93˚±17.17 for L2. For topographer B (CSP), the mean absolute rotation difference between the steep axis at 15mm reported by the topographer

and the examiner-observed rotation was 18.00˚±18.68 for L1 and 32.49˚±23.57 for L2. Figures 6 and 7 depict the distribution of observations at 15 mm for both topographers.

Figure 6: Distribution of Observations of Mean Absolute Rotation for L1 and L2 at a 15mm chord on Topographer A

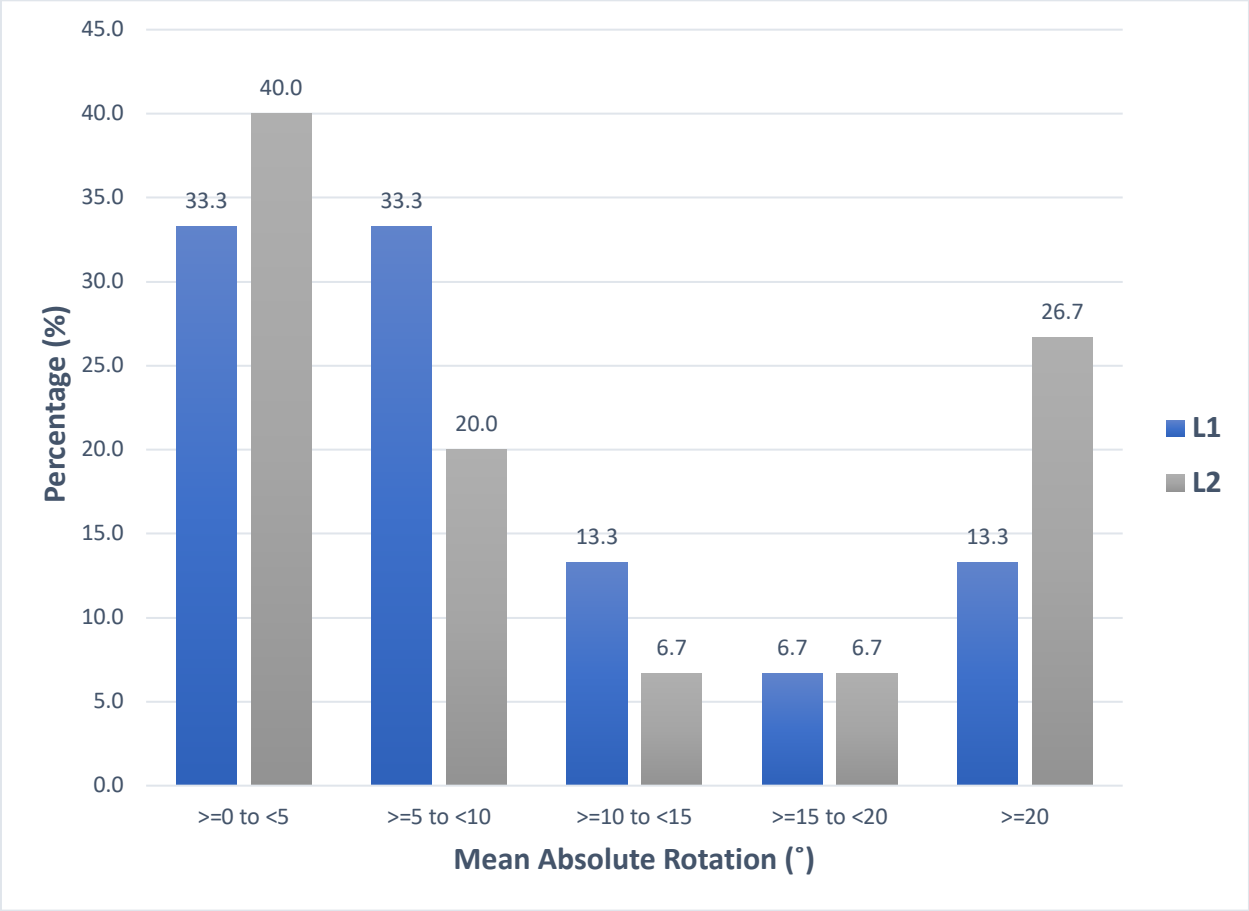

Figure 7: Distribution of Observations of Mean Absolute Rotation for L1 and L2 at a 15mm chord on Topographer B

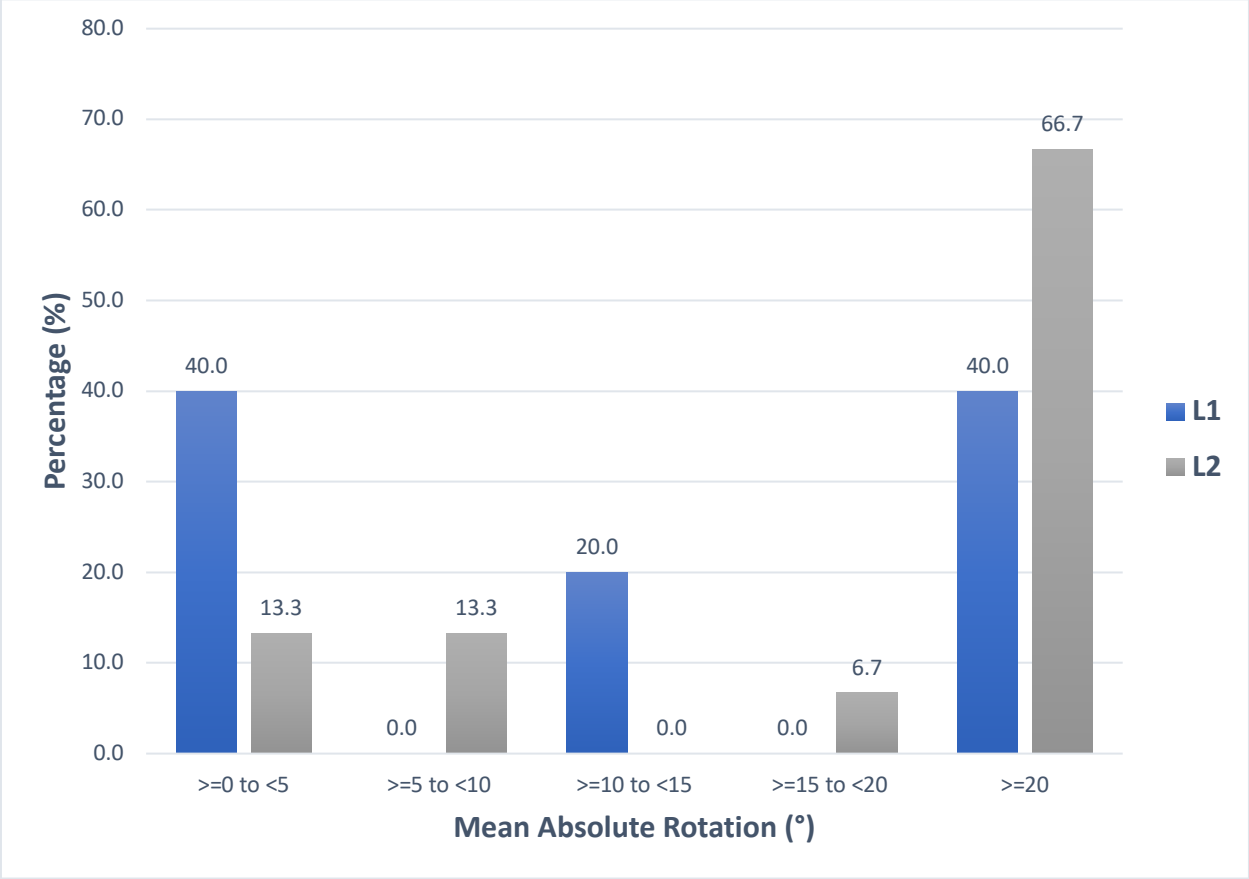

A two-way, mixed design ANOVA, with topographer as a between subjects factor and lens as a within subjects factor, yielded a non-significant topographer x lens interaction at a chord of 15mm, $F(1,14)=3.390$, $p=0.087$, $\eta^2=0.195$. Simple main effects conducted between topographer conditions revealed a significant difference between the topographers, $F(1,14)=5.437$, $p=0.035$, $\eta^2=0.280$. Simple main effects conducted between lens conditions revealed a non-significant difference between the lenses, $F(1,14)=1.981$, $p=0.181$, $\eta^2=0.124$.

When grouping the lenses together to evaluate the effect of the topographers, the mean difference in rotation for topographer A is 13.178˚±3.381 (95%CI (5.927, 20.428)) and for topographer B is 25.244˚±3.965 (95%CI (16.739, 33.749)). The mean difference between

both topographers (A – B) was 12.067˚±5.175. This difference was statistically significant according to a paired t-test (p=0.035).

4.5 Average rotation at PFD

For topographer A, the mean absolute rotation difference between the steep axis at the lens' PFD reported by the topographer and the examiner-observed rotation was 16.80˚±20.79 for L1 and 34.51˚±34.42 for L2. For topographer B, the mean absolute rotation difference between the steep axis at the lens' PFD reported by the topographer and the examiner-observed rotation was 28.22˚±34.60 for L1 and 38.11˚±31.75 for L2. Figures 8 and 9 depict the distribution of observations at the lens' PFD for both topographers.

Figure 8: Distribution of Observations of Mean Absolute Rotation for L1 and L2 at each lens' PFD on Topographer A.

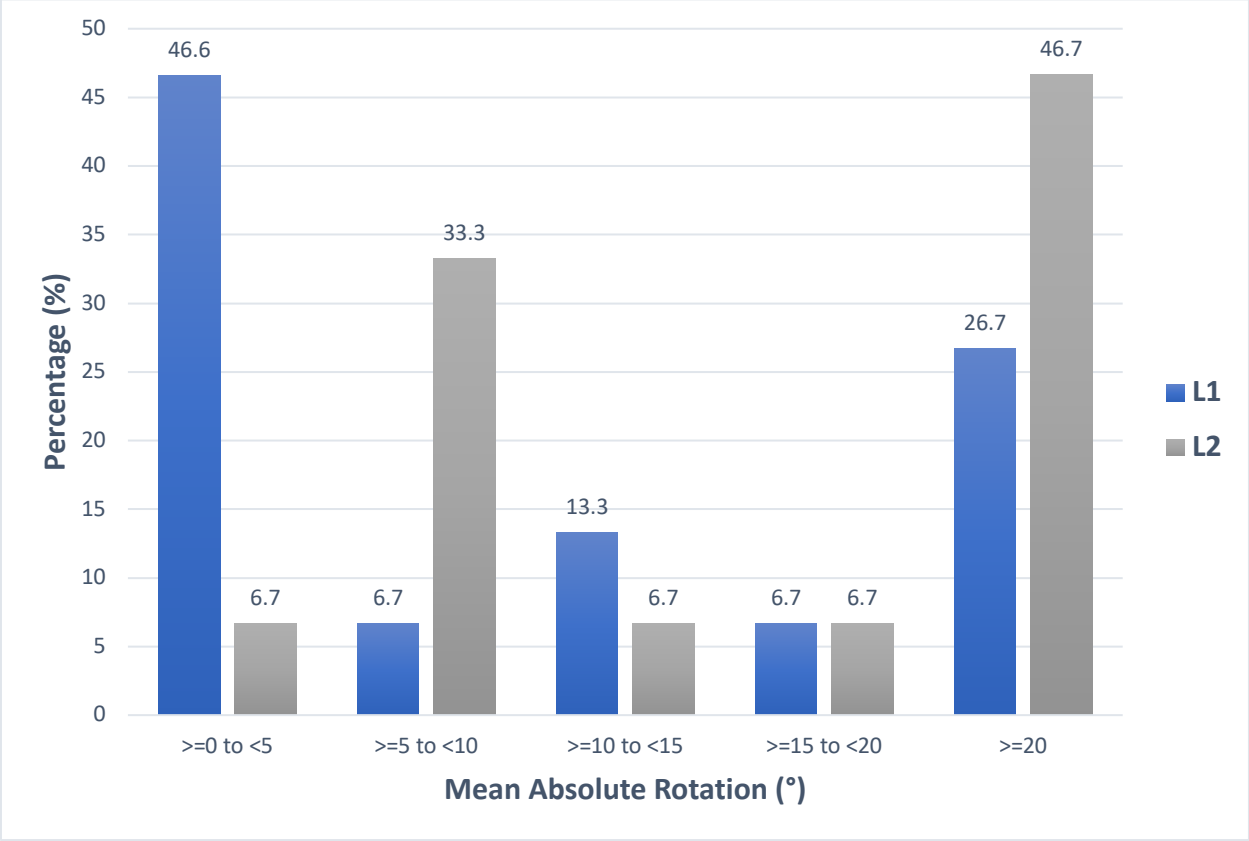

Figure 9: Distribution of Observations of Mean Absolute Rotation for L1 and L2 at each lens' PFD on Topographer B

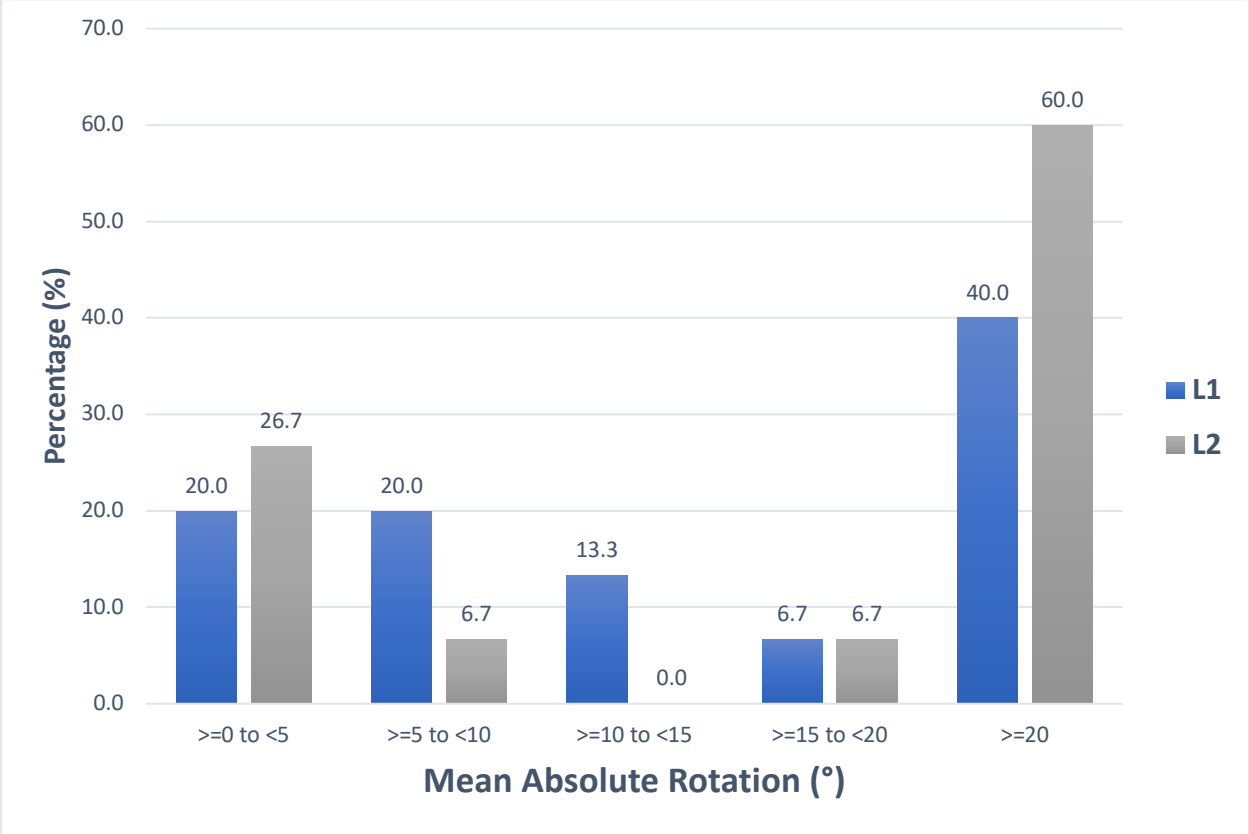

A two-way, mixed design ANOVA, with topographer as a between subjects factor and lens as a within subjects factor, yielded a non-significant topographer x lens interaction at a chord of the lens' PFD, $F(1,14)=0.513$, $p=0.486$, $\eta^2=0.035$. Simple main effects conducted between topographer conditions revealed a non-significant difference between the topographers $F(1,14)=2.896$, $p=0.111$, $\eta^2=0.171$. Simple main effects conducted between lens conditions revealed a non-significant difference between the lenses $F(1,14)=1.964$, $p=0.183$, $\eta^2=0.123$.

When grouping the lenses together to evaluate the effect of the topographers, the mean difference in rotation for topographer A is 25.655˚±5.656 (95%CI (13.524, 37.787)) and for topographer B is 33.167˚±5.661 (95%CI (21.024, 45.309)). The mean difference

between both topographers (A – B) was 7.511˚±4.414. This difference was not statistically significant according to a paired t-test (p=0.111).

4.6 Comparing Rotations at 15mm and at the lens' PFD

A paired t-test was done to compare the results of the lens' rotation at 15 mm and at the lens' PFD for both topographers. For topographer A, there was a statistically significant difference between the lens' mean difference in rotation at 15 mm and at the lens' PFD ($t(29)=-2.915$, $p<0.01$). For topographer B, there was no statistically significant difference between the lens' mean difference in rotation at 15 mm and at the lens' PFD ($t(29)=-1.618$, $p=0.117$).

4.7 Correlation Between Lens Characteristics and Mean Absolute Lens Rotation

A Pearson bivariate correlation was done between the central FRT, nasal compression and temporal compression and correlated with the mean absolute differences in rotation. A Spearman correlation was done to confirm the results. The results are presented in the tables below for L1 and L2.

Table 7: Pearson correlation between central FRT/lens compression and lens rotation for L1

		Topographer A		Topographer B	
		15mm chord	PFD	15mm chord	PFD
Central FRT (μm)	Pearson's r	-0.459	-0.322	-0.178	-0.407
	Significance (p)	0.085	0.242	0.526	0.132
	N	15	15	15	15
Nasal compression (%)	Pearson's r	-0.185	-0.162	-0.366	-0.462
	Significance (p)	0.527	0.580	0.199	0.097
	N	14	14	14	14
Temporal compression (%)	Pearson's r	0.065	0.149	0.118	0.078
	Significance (p)	0.824	0.611	0.688	0.792
	N	14	14	14	14

**p<0.05 **p<0.01 ***p<0.001*

No significant correlation was found for L1 between the lens's rotation and the three lens characteristics.

Table 8: Spearman correlation between central FRT/lens compression and lens rotation for L1

		Topographer A		Topographer B	
		15mm chord	PFD	15mm chord	PFD
Central FRT (μm)	Spearman's rho	-0.756**	-0.384	-0.116	-0.286
	Significance (p)	0.001	0.157	0.680	0.301
	N	15	15	15	15
Nasal compression (%)	Spearman's rho	-0.238	-0.253	-0.185	-0.244
	Significance (p)	0.413	0.382	0.527	0.401
	N	14	14	14	14
Temporal compression (%)	Spearman's rho	0.086	0.007	0.029	0.305
	Significance (p)	0.771	0.982	0.923	0.288
	N	14	14	14	14

**p<0.05 **p<0.01 ***p<0.001*

For L1, a Spearman's rho data analysis revealed a significant negative correlation between lens rotation at 15mm for topographer A (ρ=-0.756) and central FRT.

Table 9: Pearson correlation between central FRT/lens compression and lens rotation for L2

		Topographer A		Topographer B	
		15mm chord	PFD	15mm chord	PFD
Central FRT (μm)	Pearson's r	0.230	-0.154	-0.072	-0.319
	Significance (p)	0.410	0.584	0.798	0.246
	N	15	15	15	15
Nasal compression (%)	Pearson's r	-0.449	-0.108	0.468	-0.014
	Significance (p)	0.093	0.701	0.078	0.961
	N	15	15	15	15
Temporal compression (%)	Pearson's r	-0.359	-0.349	-0.391	0.092
	Significance (p)	0.208	0.221	0.167	0.755
	N	14	14	14	14

**p<0.05 **p<0.01 ***p<0.001*

No significant correlation was found for L2 between the lens's rotation and the three lens characteristics.

Table 10: Spearman correlation between central FRT/lens compression and lens rotation for L2

		Topographer A		Topographer B	
		15mm chord	PFD	15mm chord	PFD
Central FRT (μm)	Spearman's rho	-0.061	-0.146	-0.125	-0.250
	Significance (p)	0.829	0.603	0.657	0.368
	N	15	15	15	15
Nasal compression (%)	Spearman's rho	-0.115	-0.071	0.536*	0.014
	Significance (p)	0.684	0.800	0.040	0.960
	N	15	15	15	15
Temporal compression (%)	Spearman's rho	-0.607*	-0.398	-0.363	-0.066
	Significance (p)	0.021	0.159	0.203	0.822
	N	14	14	14	14

**p<0.05 **p<0.01 ***p<0.001*

For L2, a Spearman's rho data analysis revealed a weak significant positive correlation between lens rotation at 15mm for topographer B (ρ=-0.536) and nasal compression.

4.8 Correlation Between Ocular Surface Shape and Mean Absolute Rotation

A Pearson bivariate correlation was done between the participant's toricity and correlated with the differences in rotation. A Spearman correlation was done to confirm the results. The results are presented in the tables below.

Table 11: Pearson correlation between toricity at 3 chords and rotation of L1 and L2 for topographer A

		L1		L2	
		15mm chord	PFD	15mm chord	PFD
Toricity 14mm	Pearson's r	0.355	0.032	-0.083	-0.355
	Significance (p)	0.195	0.910	0.769	0.194
	N	15	15	15	15
Toricity 15mm	Pearson's r	-0.184	-0.367	0.180	-0.171
	Significance (p)	0.513	0.179	0.522	0.543
	N	15	15	15	15
Toricity 16mm	Pearson's r	-0.209	-0.286	0.286	-0.053
	Significance (p)	0.455	0.302	0.301	0.851
	N	15	15	15	15

**p<0.05 **p<0.01 ***p<0.001*

No significant correlation was found for topographer A between the lens's rotation and AOSS toricity.

Table 12: Spearman correlation between toricity at 3 chords and rotation of L1 and L2 for topographer A

		L1		L2	
		15mm chord	PFD	15mm chord	PFD
Toricity 14mm	Spearman's rho	-0.172	-0.291	-0.219	-0.317
	Significance (p)	0.540	0.292	0.432	0.249
	N	15	15	15	15
Toricity 15mm	Spearman's rho	-0.461	-0.526*	0.152	-0.032
	Significance (p)	0.084	0.044	0.588	0.909
	N	15	15	15	15
Toricity 16mm	Spearman's rho	-0.461	-0.564*	0.233	0.231
	Significance (p)	0.084	0.029	0.403	0.408
	N	15	15	15	15

**p<0.05 **p<0.01 ***p<0.001*

For topographer A, a Spearman's rho data analysis revealed a weak significant negative correlation between AOSS toricity at 15 mm (ρ=-0.0526) and 16 mm (ρ=-0.0564) with L1's rotation at the PFD.

Table 13: Pearson correlation between toricity at 3 chords and rotation of L1 and L2 for topographer B

		L1		L2	
		15mm chord	PFD	15mm chord	PFD
Toricity 14mm	Pearson's r	0.226	-0.022	-0.095	-0.246
	Significance (p)	0.419	0.939	0.736	0.376
	N	15	15	15	15
Toricity 15mm	Pearson's r	0.176	-0.065	-0.036	-0.077
	Significance (p)	0.531	0.818	0.899	0.786
	N	15	15	15	15
Toricity 16mm	Pearson's r	0.284	-0.040	-0.042	-0.034
	Significance (p)	0.306	0.888	0.883	0.905
	N	15	15	15	15

*$p<0.05$ $p<0.01$ $p<0.001$

No significant correlation was found for topographer B between the lens's rotation and AOSS toricity.

Table 14: Spearman correlation between toricity at 3 chords and rotation of L1 and L2 for topographer B

		L1		L2	
		15mm chord	PFD	15mm chord	PFD
Toricity 14mm	Spearman's rho	0.054	-0.307	-0.161	-0.267
	Significance (p)	0.849	0.265	0.567	0.337
	N	15	15	15	15
Toricity 15mm	Spearman's rho	0.048	-0.406	-0.138	-0.016
	Significance (p)	0.864	0.133	0.625	0.955
	N	15	15	15	15
Toricity 16mm	Spearman's rho	0.164	-0.295	-0.146	-0.066
	Significance (p)	0.558	0.286	0.603	0.815
	N	15	15	15	15

*$p<0.05$ $p<0.01$ $p<0.001$

No significant correlation was found for topographer B between the lens's rotation and AOSS toricity.

5. Discussion

The aim of this study was to determine the efficacy and accuracy of two SL topographers in their capacity to predict SL rotation. To do so, two different designs of SL were used and their rotation on the eye of each participant was compared to the steep axis of conjunctival astigmatism provided by each topographer at different chords. This information gives us much knowledge into the power and effect of empirical lens fittings and the tools necessary to improve them for the future.

The results of mean difference in rotation are significantly different for the ESP (topographer A) and the CSP (topographer B). The results at 15mm show that, for both lenses, the CSP results show higher mean differences than the CSP. The fact that there is a significant difference between the two topographers can be explained by the fact that the way the data is acquired and interpreted is different. For the ESP, the highest and lowest point of sagittal height is recorded regardless of the angle it is found at. In fact, as previously mentioned, AOSS toricity is often not regularly toric(30); in other words, it often does not respect the regular astigmatism rule of having a difference of 90˚ between meridians. Thus, this instrument accounts for irregular AOSS by providing data of the absolute highest and lowest points of the sclera at a given chord. The same data interpretation and acquisition is not true with the CSP; as an early version of this algorithm, it does provide information on AOSS. However, it assumes that the axis of astigmatism is always separated by 90˚, and there is no current way of easily extrapolating the true maximum and minimum sagittal heights at a given chord.(68) This may cause a disparity between instruments, knowing that the two extremes of sagittal height provided by the CSP may only be averages and not the true values. A recent study comparing the values of the ESP and the CSP may contribute to this conjecture. Bandlitz *et al.*(69) demonstrated that the values of maximum and minimum sagittal height were

higher with the CSP than with the ESP, however absolute AOSS toricity was higher with the ESP than with the CSP. When analyzing the mean sagittal heights and toricities of both topographers reported in this study, the results are in agreement. Although comparing the data obtained from both topographers was not the primary purpose of this study, which would have required a larger amount of participants to have accurate and statistically significant results, the similarity of these results, suggesting that both topographers do not have data that can be interchanged, may contribute to the fact that the ESP was able to have smaller results of mean absolute lens rotation than the CSP.

Examining the data on the participant's AOSS, it is interesting to note that, at a 15 mm chord on the ESP, the values for toricity were 191.33μm±74.92 for the eyes of the participants fit with the OneFit Med and 220.00μm±96.14 for the fellow eye fit with the Zenlens. This toricity describes the difference in microns between the highest and lowest point on the anterior surface regardless of their location. Unlike corneal astigmatism, these meridians are often not separated by 90˚. Knowing that the toric peripheries on both lenses used in this study were set at 150 μm, this difference may have affected how the lenses stabilized on the eye, seeing that the AOSS toricity was higher than that of the lens's peripheries. However, correlation shows that there was no relationship between the mean difference in toricity between the AOSS and the lens' toric peripheries as related to lens rotation. Knowing that the FLF's updated algorithm can now provide personalized data on the toric peripheries suited for the patient's eye, and that the toric peripheries used in this study are the standard for the trial sets in the clinic at the *Université de Montréal*, it could be interesting to duplicate this study with more custom lenses suggested by the ESP.

The mean difference in rotation results were compared at 15mm and at the lens' PFD for both topographers regardless of the lens studied. There was a significant difference in values for the ESP, however the values for the CSP were not significantly different. This difference can be explained by the fact that both topographers, as explained above, do not deliver their information in a similar manner which may affect the reliability of the

results of rotation. The mean differences in rotation for the CSP were always higher than those for the ESP regardless of the lens studied. This could be explained by the fact that the CSP has a harder time identifying the steep meridian on the sclera, the place where the lens will stabilize. Because of this, the CSP has been demonstrated to be a weaker predictor of SL rotation. However, the significant difference between both chords for the ESP is also an interesting result. The PFD of the lens is a characteristic specific to each lens which denotes the first point of contact between the lens and the ocular surface. In this case, the PFD of the OneFit MED lens of a 15.6 mm diameter was 13.6mm and that of the Zenlens of a 16 mm diameter was 12.8mm. Given the fact that we know that the AOSS becoming increasingly toric as of a chord of 15mm, the ocular surface may not be sufficiently toric at the chords of the PFD of the given lenses to provide enough information about lens rotation. It would therefore be clinically relevant to reproduce this study with larger diameter lenses (i.e. 18 mm or 20 mm), whose PFD are equal to or greater than 15 mm.

In this study, lenses were chosen based on the First Lens Fit (FLF) algorithm on the ESP. While this was not the primary goal of the study, it is interesting to evaluate the accuracy in which this algorithm can predict the first lens that will be suitable on the patient's eye. This is done in part by looking at lens rotation but can also be done by looking at the FRT. The fitting guides of both the OneFit Med(66) and the Zenlens(67) suggest a 200-225 micron and 300-micron FRT 30 minutes after lens insertion, respectively. For the OneFit MED lens, although the mean FRT is slightly less than this amount (189.20±82.76 μm, SE = 21.37, 95%CI(143.37,235.03)), the 200-225 μm range is within the confidence interval, deeming a seemingly successful lens prediction based on FRT. Conversely, the FRT of the Zenlens predicted by the FLF algorithm was much higher than the fitting guide suggests (405.67±113.40 μm, SE = 29.28, 95%CI(342.87,468.47)) and the suggested FRT in the fitting guide was not a value found in the confidence interval. This demonstrates that the ESP tends to overshoot the FRT for the Zenlens by about 100 μm. However, it is clinically interesting to note that there were outliers in both lens groups that could have skewed the means. For example, the minimum value for the OneFit MED lens

had a central FRT of 64 microns, which is not clinically acceptable, and the Zenlens had a maximum value of 598 microns, which is clinically inacceptable as well.

An interesting finding in this study is that the FRT was not significantly correlated with lens rotation. This was surprising to the authors, seeing as a common clinical assumption with SL fittings is that lenses with a higher FRT have a tendency to move more on the surface of the eye, therefore causing decreased stability, which is undesirable in successful fittings and which also make it difficult to evaluate a stable lens rotation(65). In a clinical setting, with lenses that have a FRT that is too high from the suggested value, the clinician's reflex is to instantly change the lens for one that is closer to the target FRT. This incidental finding demonstrates that we can rely on our measurement of rotation regardless of central FRT, which also implies that we can order a new lens based off of a previous lens even if its FRT was inadequate. Evidently it is important to note that the maximum value of central FRT was 598 μm for the Zenlens and 325 μm for the OneFit MED, therefore this result may not translate to higher FRT or other lens designs than those used in this study. Even more, the FLF algorithm has evolved since the conception of this study and now includes suggested peripheral curves based on the patient's AOSS toricity. In the future, it would be clinically relevant to further evaluate the capacities of this advanced software.

It is interesting to note that 80% of observations for the OneFit Med and 66.7% of observations for the Zenlens had mean absolute rotation differences smaller than 15˚ using the Eaglet at a 15 mm chord. As previously mentioned, in a SL context, the accurate prediction of SL rotation plays a crucial role in obtaining precise visual outcomes when prescribing front-toric lenses. This is an interesting clinical tool, however, since there are no current studies evaluating SL rotation, it is clinically relevant to parallel this concept with the rotation of soft toric lenses.

It has been noted in the literature that 5˚ of axis misalignment can decrease visual quality.(70) Other authors(71) have explained that the greatest and most significant loss in visual acuity comes between 10˚ and 20˚ of misalignment. A study(58) investigating

the effect of the misalignment of cylinder axis in soft contact lens wearers with over 0.75D of astigmatism demonstrated that axis misalignment, also referred to as lens rotation, had a different effect depending on the amount of astigmatism. Cylinder axis misalignment for participants with higher amount of astigmatism (over 2.00D astigmatism) was less tolerated. However, all groups of astigmatism noted a significant effect of axis misalignment on high/low contrast visual acuity, vision clarity and satisfaction but a non-significant effect on vision acceptability. Participants in this study with low amounts of astigmatism (between 0.75D and 1.25D) displayed stable VA between a misalignment of +30˚ to -30˚, with medium amounts of astigmatism (1.25D – 2.00D) had stable VA between an axis misalignment of +10° to -10˚ and the high astigmatism group (over 2.00D) did not tolerate any amount of misalignment. The results of the previously described study highlight knowledge that is extremely well known in a clinical setting about soft toric contact lenses: a lens with an astigmatism of 0.75 D can tolerate 15˚ of rotation. However, the higher the amount of toricity, the more important it is for the lens to remain stable and have little to no rotation for vision to remain clear. In this case, a rotation of 15˚ becomes clinically inacceptable.

Therefore, it is difficult to determine a clinically acceptable amount of rotation because this depends on the amount of prescribed front-toricity. In research published by Lindsay *et al.*(72) about calculating induced astigmatic power from lens rotation, the authors demonstrated that an increased amount of lens rotation will cause higher amounts of induced astigmatism, increasing exponentially with higher amounts of astigmatic correction (see figure 10 below). Clinically speaking, a lens with a toricity of 0.75 D will tolerate up to 20˚ of misalignment.(73) However, only 5˚ of rotation can be tolerated for cylinder power equal to or greater than 1.50 D. Knowing this information, higher amounts of cylinder require more specific fits and may therefore not be suited for the ESP's empirical technology at this point in time.

Figure 10: Induced Astigmatism with Rotation of Soft Toric Contact Lenses (74)

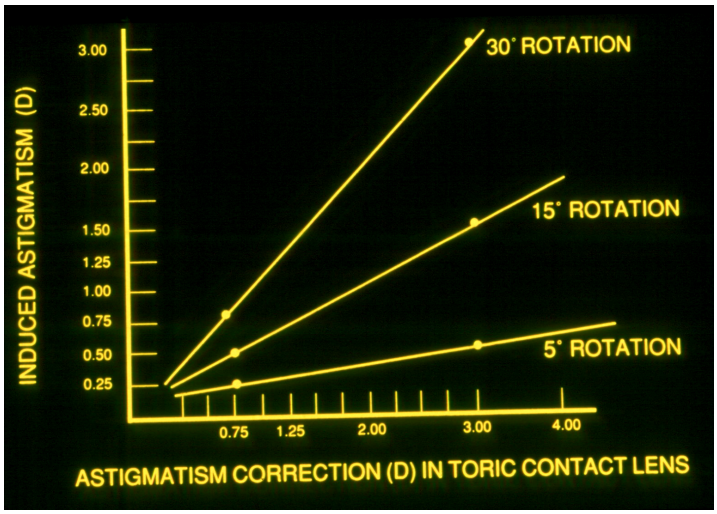

This study design evaluating lens rotation is a novel concept in SL research; thus, there are few comparable studies published in the literature today. However, these findings are similar to those noted by Rojas *et al.*(75) in their scientific poster, who found a mean absolute difference in lens rotation of 16˚±14 using the ESP and at the same chord. However, the previous study did not distinguish between lenses as their goal was to evaluate if changes in back-surface toricity on SL impacted the way a lens will settle on the ocular surface. As well, instead of using the steep meridian as their axis of reference, they referred to the flat meridian for lens rotation. Their findings suggested that eyes with higher amounts of conjunctival toricity, which inevitably require lenses with larger amounts of prescribed back-surface toricity (i.e. greater than 200 microns of difference) will settle more accurately than lenses with lower prescribed toricities settling on less toric eyes. However, the back-surface toricities used in the current study were identical for both lenses (150 microns) as the goal of this study was to evaluate whether one topographer or another can, and if so, is better equipped to predict lens rotation.

However, one variable that can be compared between the two studies is the mean absolute lens rotation the author's reported for SL with back surface toricities between 126 and 200 microns inclusively, which was 14˚±13. In the present study, the mean absolute difference in rotation of the examiner-observed rotation as compared with the

steep axis of conjunctival astigmatism at 15mm on the ESP was noted as 12.42˚±16.93 for the OneFit Med and 13.93˚±17.17 for the Zenlens. Although the lenses used in both studies are different (OneFit Med and Zenlens in the present study, ICD Flexfit and Zenlens in the study by Rojas *et al.*), these results are comparable to a certain degree. It is important to note, however, that while the current study measured observed lens rotation based on the steep axis of both the lens and the ocular surface, Rojas *et al.* measured rotation based on the flat axis of the lens and the conjunctiva. As well, the aforementioned study was done on eyes with ectasia, and as previously mentioned, ectatic eyes have different AOSS than those with normal corneas, who were used in this study. Moreover, Rojas *et al.* used a computer software to evaluate lens rotation whereas the main author of this study evaluated lens rotation at the slit lamp. Although it is impossible to say that both study results are identical and in agreement since their methodologies are different, it remains clinically relevant to parallel these studies in order to survey the research available on this topic to date. Further studies with comparable methodologies are required to have repeatable and comparable literature on lens rotation.

It was also hypothesized that lens compression would impact lens rotation. This hypothesis is based on the assumption that lenses that are more compressed on the conjunctiva will have less of a tendency to rotate and stabilize on the ocular surface's flat and steep meridians. Visser *et al.* demonstrated in their study on toric SL that lens rotation is lessened at the end of the day due to the fact that the lens is more compressed into the conjunctiva.(54) The results of this study demonstrate that, although there was a statistically significant difference in lens compression between both lenses (more temporal compression resulting from a lens that was decentered mostly temporally), this compression, neither nasal nor temporal, was correlated with lens rotation. Nevertheless, while these study results suggest that lens rotation is not correlated with lens compression, it could be interesting to validate these results by studying the effect of induced, inacceptable lens compression and lens edge elevation on lens rotation.

Finally, potential biases that could have affected the results of this study are in part due to the fact that the examiner-observed rotation was done at the slit lamp. The authors are

aware that this may have diminished the precision of the measurements since the gradation of axis values on the slit lamp is in 5˚ increments. Other computer softwares are able to calculate lens rotation with a decimal precision on the degree value, which would have been extremely precise. However, the method at the slit lamp was chosen to remain true to the observed rotation that clinicians perform in their practices therefore obtaining the most clinically relevant results. Moreover, a secondary, masked observer would have been ideal to partially remedy this situation by ensuring data repeatability, however this was not possible for the present study due to lack of resources and manpower. The data collection for this study was done directly following the approval of the commencement of research activities at the *Clinique Universitaire de la Vision* after the first COVID-19 lockdown. Minimal on-site presence was allowed for research projects seeing as the staff and clinical personnel were encouraged to remain off campus as much as possible. While a secondary observer was planned and part of the protocol at the time that this project was submitted to the CERC, whose role was to validate lens rotation as well as re-measure anterior segment OCTs to ensure repeatability, the sanitary crisis restrictions made this impossible to achieve. Also, initially at lens application, the lens markings were rotated to the horizontal meridian and the rotation was then measured after 30 minutes. Another aspect that could have been added to further validate the predictability and stability of lens rotation would have been to apply a second manual rotation after 30 minutes by about 45˚ and execute a second measurement. Moreover, the small sample size could have affected the results, seeing as data that was non-significant in this study may have become significant with a much larger number of participants. Even more, the ESP is dependent on fluorescein to obtain a proper measurement; however, there exists no current standardized method to ensure that the participant always had the same amount of fluorescein on the ocular surface, which may have influenced the data from this instrument. Finally, since this study was carried out with two lens designs, its results cannot be generalized to all types of scleral lenses and only apply to those used here and with this study population.

6. Conclusion

In conclusion, the ESP and the CSP are interesting clinical tools to map anterior ocular surface shape. However, both their predictions of lens rotation are not comparable at this time. Although the image acquisition process for CSP is easier to use since it does not require the use of sodium fluorescein and it is non-invasive, its prediction of lens rotation is not accurate and therefore not applicable in clinic. The ESP was able to predict lens rotation within less than 15˚ from slit lamp observation, deeming this instrument clinically acceptable for lenses with low cylinder values. However, lenses necessitating high amounts of front-surface toricity and customized fits may not be suited for the empirical fitting technology today, since this rotation may cause a significant reduction in visual acuity.

References

1. Pearson RM, Efron N. Hundredth anniversary of August Müller's inaugural dissertation on contact lenses. Survey of ophthalmology. 1989;34(2):133-41.
2. Fick AE. A contact-lens. 1888 (translation). Archives of ophthalmology (Chicago, Ill : 1960). 1988;106(10):1373-7.
3. Bowden T. Contact Lenses: The Story. Kent: Bower House Publications; 2009.
4. Pearson RM. Kalt, keratoconus, and the contact lens. Optom Vis Sci. 1989;66(9):643-6.
5. Schein OD, Rosenthal P, Ducharme C. A gas-permeable scleral contact lens for visual rehabilitation. American journal of ophthalmology. 1990;109(3):318-22.
6. Ezekiel D. Gas permeable haptic lenses. Journal of The British Contact Lens Association. 1983;6(4):158-61.
7. Pullum KW. The unique role of scleral lenses in contact lens practice. Cont Lens Anterior Eye. 1999;22 Suppl 1:S26-34.
8. Visser ES, Visser R, van Lier HJ, Otten HM. Modern scleral lenses part II: patient satisfaction. Eye Contact Lens. 2007;33(1):21-5.
9. Vincent SJ, Alonso-Caneiro D, Collins MJ. Miniscleral lens wear influences corneal curvature and optics. Ophthalmic Physiol Opt. 2016;36(2):100-11.
10. Soeters N, Visser ES, Imhof SM, Tahzib NG. Scleral lens influence on corneal curvature and pachymetry in keratoconus patients. Cont Lens Anterior Eye. 2015;38(4):294-7.
11. Gungor I, Schor K, Rosenthal P, Jacobs DS. The Boston Scleral Lens in the treatment of pediatric patients. Journal of AAPOS : the official publication of the American Association for Pediatric Ophthalmology and Strabismus. 2008;12(3):263-7.
12. van der Worp E, Bornman D, Ferreira DL, Faria-Ribeiro M, Garcia-Porta N, Gonzalez-Meijome JM. Modern scleral contact lenses: A review. Cont Lens Anterior Eye. 2014;37(4):240-50.
13. Shorter E, Harthan J, Nau CB, Nau A, Barr JT, Hodge DO, et al. Scleral Lenses in the Management of Corneal Irregularity and Ocular Surface Disease. Eye Contact Lens. 2018;44(6):372-8.
14. Weyns M, Koppen C, Tassignon MJ. Scleral contact lenses as an alternative to tarsorrhaphy for the long-term management of combined exposure and neurotrophic keratopathy. Cornea. 2013;32(3):359-61.
15. Galor A, Zlotcavitch L, Walter SD, Felix ER, Feuer W, Martin ER, et al. Dry eye symptom severity and persistence are associated with symptoms of neuropathic pain. Br J Ophthalmol. 2015;99(5):665-8.
16. Keating AM, Jacobs DS. Anti-VEGF Treatment of Corneal Neovascularization. Ocul Surf. 2011;9(4):227-37.
17. Kalwerisky K, Davies B, Mihora L, Czyz CN, Foster JA, DeMartelaere S. Use of the Boston Ocular Surface Prosthesis in the management of severe periorbital thermal injuries: a case series of 10 patients. Ophthalmology. 2012;119(3):516-21.

18. Ciralsky JB, Chapman KO, Rosenblatt MI, Sood P, Fernandez AG, Lee MN, et al. Treatment of Refractory Persistent Corneal Epithelial Defects: A Standardized Approach Using Continuous Wear PROSE Therapy. Ocul Immunol Inflamm. 2015;23(3):219-24.
19. Fadel D. Modern scleral lenses: Mini versus large. Cont Lens Anterior Eye. 2017;40(4):200-7.
20. Michaud L, Lipson M, Kramer E, Walker M. The official guide to scleral lens terminology. Cont Lens Anterior Eye. 2020;43(6):529-34.
21. Fadel D. Scleral Lens Issues and Complications Related to a Non-optimal Fitting Relationship Between the Lens and Ocular Surface. Eye Contact Lens. 2019;45(3):152-63.
22. Courey C, Michaud L. Variation of clearance considering viscosity of the solution used in the reservoir and following scleral lens wear over time. Cont Lens Anterior Eye. 2017;40(4):260-6.
23. Hall L. What You Need to Know About Sagittal Height and Scleral Lenses. Contact Lens Spectr [Internet]. 2015.
24. Fuller DG, Wang Y. Safety and Efficacy of Scleral Lenses for Keratoconus. Optom Vis Sci. 2020;97(9):741-8.
25. Barnett M, Fadel D. Scleral Lenses: Prepare for Landing. Contact Lens Spectr [Internet]. 2017.
26. Johns L. Using toricity with scleral lenses. Optometry Times [Internet]. 2016.
27. van der Worp E, Mertz C. Sagittal height differences of frequent replacement silicone hydrogel contact lenses. Cont Lens Anterior Eye. 2015;38(3):157-62.
28. Fadel D. The influence of limbal and scleral shape on scleral lens design. Cont Lens Anterior Eye. 2018;41(4):321-8.
29. Hall LA, Hunt C, Young G, Wolffsohn J. Factors affecting corneoscleral topography. Invest Ophthalmol Vis Sci. 2013;54(5):3691-701.
30. DeNaeyer G, Sanders D, VanDerWorp E, Jedlicka J, Michaud L, Morrison S. Qualitative Assessment of Scleral Shape Patterns Using a New Wide Field Ocular Surface Elevation Topographer. Journal of Contact Lens Research and Science. 2017.
31. DeNaeyer G, Sanders D, Michaud L, Morrison S, Walker M, Jedlicka J, et al. Correlation of Corneal and Scleral Topography in Cases with Ectasias and Normal Corneas. Journal of Contact Lens Research and Science. 2019.
32. Consejo A, Rozema JJ. Scleral Shape and Its Correlations With Corneal Astigmatism. Cornea. 2018;37(8):1047-52.
33. Worp EVD, Graf T, Caroline P. Exploring Beyond the Corneal Borders. Contact Lens Spectr [Internet]. 2010.
34. Hall LA, Young G, Wolffsohn JS, Riley C. The influence of corneoscleral topography on soft contact lens fit. Invest Ophthalmol Vis Sci. 2011;52(9):6801-6.
35. Kowalski LP, Collins MJ, Vincent SJ. Scleral lens centration: The influence of centre thickness, scleral topography, and apical clearance. Cont Lens Anterior Eye. 2020;43(6):562-7.
36. Iskander DR, Wachel P, Simpson PN, Consejo A, Jesus DA. Principles of operation, accuracy and precision of an Eye Surface Profiler. Ophthalmic Physiol Opt. 2016;36(3):266-78.
37. Jesus DA, Kedzia R, Iskander DR. Precise measurement of scleral radius using anterior eye profilometry. Cont Lens Anterior Eye. 2017;40(1):47-52.

38. Wolffsohn JS, Morgan PB, Barnett M, Downie LE, Jacobs DS, Jones L, et al. Contact Lens Evidence-Based Academic Reports (CLEAR). Cont Lens Anterior Eye. 2021;44(2):129-31.
39. Garner LF. Sagittal height of the anterior eye and contact lens fitting. Am J Optom Physiol Opt. 1982;59(4):301-5.
40. Vincent SJ, Alonso-Caneiro D, Collins MJ. The temporal dynamics of miniscleral contact lenses: Central corneal clearance and centration. Cont Lens Anterior Eye. 2018;41(2):162-8.
41. Otchere H, Jones LW, Sorbara L. Effect of Time on Scleral Lens Settling and Change in Corneal Clearance. Optom Vis Sci. 2017;94(9):908-13.
42. Alonso-Caneiro D, Vincent SJ, Collins MJ. Morphological changes in the conjunctiva, episclera and sclera following short-term miniscleral contact lens wear in rigid lens neophytes. Cont Lens Anterior Eye. 2016;39(1):53-61.
43. Vincent SJ, Alonso-Caneiro D, Collins MJ. Optical coherence tomography and scleral contact lenses: clinical and research applications. Clin Exp Optom. 2019;102(3):224-41.
44. Walker MK, Bergmanson JP, Miller WL, Marsack JD, Johnson LA. Complications and fitting challenges associated with scleral contact lenses: A review. Cont Lens Anterior Eye. 2016;39(2):88-96.
45. Schornack MM, Fogt J, Harthan J, Nau CB, Nau A, Cao D, et al. Factors associated with patient-reported midday fogging in established scleral lens wearers. Cont Lens Anterior Eye. 2020;43(6):602-8.
46. Denaeyer G. Strategies for decreasing the impact of scleral Lens debris. Contact Lens Spectr [Internet]. 2011.
47. Postnikoff CK, Pucker AD, Laurent J, Huisingh C, McGwin G, Nichols JJ. Identification of Leukocytes Associated With Midday Fogging in the Post-Lens Tear Film of Scleral Contact Lens Wearers. Invest Ophthalmol Vis Sci. 2019;60(1):226-33.
48. Denaeyer G, Michaud L. Scleral Lens Troubleshooting: What to do when something goes wrong with scleral lenses. Contact Lens Spectr [Internet]. 2017.
49. Fisher D, Collins MJ, Vincent SJ. Conjunctival prolapse during open eye scleral lens wear. Cont Lens Anterior Eye. 2021;44(1):115-9.
50. Courey C, Courey G, Michaud L. Conjunctival Inlapse: Nasal and Temporal Conjuctival Shape Variations associated with Scleral Lens Wear. Journal of Contact Lens Research and Science. 2018.
51. Severinsky B, Behrman S, Frucht-Pery J, Solomon A. Scleral contact lenses for visual rehabilitation after penetrating keratoplasty: long term outcomes. Cont Lens Anterior Eye. 2014;37(3):196-202.
52. Vincent SJ, Fadel D. Optical considerations for scleral contact lenses: A review. Cont Lens Anterior Eye. 2019;42(6):598-613.
53. Marsack JD, Ravikumar A, Nguyen C, Ticak A, Koenig DE, Elswick JD, et al. Wavefront-guided scleral lens correction in keratoconus. Optom Vis Sci. 2014;91(10):1221-30.
54. Visser ES, Visser R, Van Lier HJ. Advantages of toric scleral lenses. Optom Vis Sci. 2006;83(4):233-6.
55. Visser ES, Van der Linden BJ, Otten HM, Van der Lelij A, Visser R. Medical applications and outcomes of bitangential scleral lenses. Optom Vis Sci. 2013;90(10):1078-85.

56. Nau CB, Schornack MM. Region-Specific Changes in Postlens Fluid Reservoir Depth Beneath Small-Diameter Scleral Lenses Over 2 Hours. Eye Contact Lens. 2018;44 Suppl 1:S210-s5.
57. Michaud L, Courey G. Influence of the Scleral Lens and Fluid Reservoir Thicknesses on Residual Astigmatism. Journal of Contact Lens Research and Science. 2021.
58. Sha J, Fedtke C, Tilia D, Yeotikar N, Jong M, Diec J, et al. Effect of cylinder power and axis changes on vision in astigmatic participants. Clinical optometry. 2019;11:27-38.
59. Applegate RA, Hilmantel G, Howland HC, Tu EY, Starck T, Zayac EJ. Corneal first surface optical aberrations and visual performance. J Refract Surg. 2000;16(5):507-14.
60. Applegate RA, Howland HC, Sharp RP, Cottingham AJ, Yee RW. Corneal aberrations and visual performance after radial keratotomy. J Refract Surg. 1998;14(4):397-407.
61. Young G, Hunt C, Covey M. Clinical evaluation of factors influencing toric soft contact lens fit. Optom Vis Sci. 2002;79(1):11-9.
62. Briggs S, Bin Moammar M. Effect of 2% fluorescein on Scheimpflug central corneal thickness measurements. Int J Ophthalmol. 2016;9(2):239-42.
63. Barnett M, Courey C, Fadel D, Lee K, Michaud L, Montani G, et al. CLEAR - Scleral lenses. Contact Lens and Anterior Eye. 2021;44(2):270-88.
64. FAQ [Available from: https://www.carlobenedetti.it/en/f-a-q/.
65. Van Der Worp E. A guide to scleral lens fitting. Scleral Lens Education Society; 2010.
66. OneFit MED Fitting Guide. Blanchard Laboratories, Sherbrooke, Quebec.
67. Zenlens Fitting Guide.
68. Carver M. Information about Max/Min Sag Height Values on the CSP. In: Courey G, editor. Personal Communication2021.
69. Bandlitz S, Esper P, Stein M, Dautzenberg T, Wolffsohn JS. Corneoscleral Topography Measured with Fourier-based Profilometry and Scheimpflug Imaging. Optom Vis Sci. 2020;97(9):766-74.
70. Pujol J, Arjona M, Arasa J, Badia V. Influence of amount and changes in axis of astigmatism on retinal image quality. J Opt Soc Am A Opt Image Sci Vis. 1998;15(9):2514-21.
71. Tognetto D, Perrotta AA, Bauci F, Rinaldi S, Antonuccio M, Pellegrino FA, et al. Quality of images with toric intraocular lenses. J Cataract Refract Surg. 2018;44(3):376-81.
72. Lindsay R, Bruce A, Brennan N, Pianta M. Determining axis misalignment and power errors of toric soft lenses. International Contact Lens Clinic. 1997.
73. Quinn T. Soft Toric Rotation: How Much is Too Much? Contact Lens Spectr [Internet]. 2009.
74. Russel B, editor Toric Clinical Skills. The Vision Care Institue; 2006; Jacksonville, Florida.
75. Rojas J, Sebastian J, Stortelder R. Back-Surface Toric Scleral Lens Stabilization as a Function of the Amount of Toricity. Global Specialty Lens Symposium; Las Vegas2020.

Annexe

1. Inclusion and Exclusion Criteria

Inclusion	Exclusion
- Must be between 18 and 45 years of age - Must present normal ocular health. - Must not have worn regular contact lenses for the past 48 hours - Must be legally able to provide free and informed consent to participate in this study. - Must be available for one experimental session.	- Must not have an active ocular infection or disease at the moment of the clinical trials that could impact visual acuity. - Must not have corneal ectasia, corneal scarring or irregularities - Must not be currently using topical medication. - Must not have a known hypersensitivity or allergy to the products used during this trial. - Must not be a gas permeable lens wearer, small or sclerals.